Pharm Res (2014) 31:1219–1238
DOI 10.1007/s11095-013-1244-8

RESEARCH PAPER

Bicontinuous Cubic Liquid Crystalline Nanoparticles for Oral Delivery of Doxorubicin: Implications on Bioavailability, Therapeutic Efficacy, and Cardiotoxicity

Nitin K. Swarnakar • Kaushik Thanki • Sanyog Jain

Received: 27 July 2013 / Accepted: 20 October 2013 / Published online: 12 November 2013

ABSTRACT

Purpose The present study explores the potential of bicontinous cubic liquid crystalline nanoparticles (LCNPs) for improving therapeutic potential of doxorubicin.

Methods Phytantriol based Dox-LCNPs were prepared using hydrotrope method, optimized for various formulation components, process variables and lyophilized. Structural elucidation of the reconstituted formulation was performed using HR-TEM and SAXS analysis. The developed formulation was subjected to exhaustive cell culture experiments for delivery potential (Caco-2 cells) and efficacy (MCF-7 cells). Finally, *in vivo* pharmacokinetics, pharmacodynamic studies in DMBA induced breast cancer model and cardiotoxicity were also evaluated.

Results The reconstituted formulation exhibited Pn3m type cubic structure, evident by SAXS and posed stability in simulated gastrointestinal fluids and at accelerated stability conditions for 6 months. Dox-LCNPs revealed significantly higher cell cytotoxicity (16.23-fold) against MCF-7 cell lines as compared to free drug owing to its preferential localization in the vicinity of nucleus. Furthermore, Caco-2 cell experiments revealed formation of reversible "virtual pathways" in the cell membrane for Dox-LCNPs and hence posed significantly higher relative oral bioavailability (17.74-fold). Subsequently, Single dose of Dox-LCNPs (*per oral*) led to significant reduction in % tumor burden (~42%) as compared that of ~31% observed in case of Adriamycin® (*i.v.*) when evaluated in DMBA induced breast cancer model. Moreover, Dox induced cardiotoxicity was also found to be significantly lower in case of Dox-LCNPs as compared to clinical formulations (Adriamycin® and Lipodox®).

Conclusion Incorporation of Dox in the novel LCNPs demonstrated improved antitumor efficacy and safety profile and can be a viable option for oral chemotherapy.

KEY WORDS cardiotoxicity · doxorubicin · liquid crystalline nanoparticles (LCNPs) · oral delivery · Phytantriol

INTRODUCTION

Doxorubicin (Dox), one of the most potent anticancer drugs is prescribed for the treatment of wide range of cancers. Clinically approved Dox formulations (Adriamycin® and Rubex®) are rapidly cleared from the central compartment to non-specific tissue compartment within 5 min upon intravenous administration leading to sub-therapeutic levels in plasma and also necessitates frequent administration (1). Direct exposure of potent drug to the tissue also leads to serious side effect such as irreversible cardiomyopathy, myelosuppression etc. Although, novel delivery strategies such as PEGylated liposomes (Doxil, LipoDox®) have been implemented to enhance circulation half-life, these clinically available formulations are intended for intravenous administration (*i.v.*) only and often associated with poor patient compliance and other clinical complications such as hand-foot syndrome apart from side effects classical to Dox and may lead to early termination of the therapy (2,3). Peroral route is the safest route of drug administration which has higher patient compliance, lesser complications and cost-effectiveness as compared to parental drug delivery. Oral delivery of Dox, although fascinating, is often associated with poor oral bioavailability (<5%) due to its inherent low permeability, substrate specificity to P-gp efflux pump and susceptibility for extensive high first pass metabolism (4,5).

Electronic supplementary material The online version of this article (doi:10.1007/s11095-013-1244-8) contains supplementary material, which is available to authorized users.

N. K. Swarnakar • K. Thanki • S. Jain (✉)
Centre for Pharmaceutical Nanotechnology, Department of Pharmaceutics
National Institute of Pharmaceutical Education and Research (NIPER)
Sector 67, S.A.S. Nagar, Mohali, Punjab 160062, India
e-mail: sanyogjain@niper.ac.in; sanyogjain@rediffmail.com

Over the last few years, drug delivery via carrier based approaches such as either lipidic carrier or polymeric carrier and co-administration of Dox and other bioactives such as enzyme/P-gp inhibitors, quercetin, morin, cyclosporin A etc. have been implemented (6). Although, these techniques were successful up to some extent, these do suffer from one or more limitations such as poor drug loading, complex manufacturing process, insufficient bioavailability and certain immunological or medical complications (7). At present, none of formulations was found to be orally efficient and clinically pertinent. Our group is also actively involved in development various novel formulations for oral delivery of Dox. Orally administered Dox-loaded poly(lactic-co-glycolic acid) (PLGA) nanoparticles demonstrated significant tumor growth inhibition in 7, 12-dimethylbenz[α]anthracene (DMBA) induced breast cancer model in the rats which was equivalent to that of free Dox (*i.v.*) (5). Further, a patented Dox loaded layersomes technologies also exhibited significant reduction in the tumor growth as compared to control and free Dox (*i.v.*), while results were comparable to LipoDox® (*i.v.*). However, its multiple dosing was required to demonstrate anticancer activity (8).

Over the last few years, liquid crystalline nanoparticles (LCNPs) have been identified as promising oral drug delivery vehicle (6). The LCNPs are self-assembled structure, formed upon exposing polar lipids into polar environment in presence of suitable surfactant. These assemblies demonstrate existence of non-lamellar structure consisting of hydrophilic and lipophilic domains (9). The special arrangement of lipids provides both rigid and fluidic characteristics thereby imparting stability, sustained release profile and high drug payload to the system (10,11). Therefore, LNCPs transforms into various secondary vehicles (mixed micelles, cubic and hexagonal nanoparticles, vesicular carriers) in the gastrointestinal (GI) tract. In spite of their transformation, LCNPs are able to hold the drug inside the matrix and are believed to facilitate the absorption of drugs via various mechanisms such as membrane fusing properties, receptor mediated endocytosis, absorption transporters, etc. (10,11). Enhancement in oral bioavailability of few drugs such as such as omapatrilat, simvastatin, silymarin etc. has been reported via incorporation into LCNPs (12–17).

Phytantriol, is a newer generation of lipid categorized under the generally recognized as safe (GRAS) substance, has been explored for the preparation of LCNPs (18–20). In contrast to glyceride lipids, it is non-digestible lipid that provides superior encapsulation, improved GI stability, and sustained release behavior of encapsulated bioactives (15,17). Boyd and coworkers have demonstrated about 7.0-fold higher oral bioavailability of cinnarizine by phytantriol based LNCPs (15). However, none of report till date has explored their potential in improving the therapeutic efficacy and safety profile of anticancer drugs following oral administration.

In present work, Dox loaded phytantriol based LNCPs have been prepared, extensively optimized for formulation components and process parameters. Then after, formulation was freezed dried by employing step-wise freeze drying cycle for enhancing its storage stability. The developed formulation was characterized by various *in vitro* techniques. Finally, delivery potential of Dox-LCNPs was evaluated by extensive *in vitro* cell culture experiments and *in vivo* pharmacokinetic, antitumor efficacy and cardiotoxicity studies following oral administration and comparison with *i.v.* administered marketed formulations of Dox i.e. Adriamycin® and LipoDox®.

MATERIALS AND METHODS

Doxorubicin hydrochloride salt (>99%), 3,7,11,15-tetramethyl-1,2,3-hexadecanetriol (phytantriol), different grades of Pluronic® (F-108, F-127, F-68 and F-87) and cyclosporin A were generous gift from Sun Pharma Advanced Research Company (SPARC Ltd.), Vadodara, India, DSM Nutritional Products, Inc., Germany, BASF, Germany and Panacea Biotech, Mumbai, India, respectively. Triton X-100, 12-dimethylbenz[a]anthracene (DMBA), sulforhodamine B dye (SRB), Neutral red (NR), 4′,6-diamidino-2-phenylindole (DAPI) and Minimum Essential Medium Eagle (MEM) were purchased from Sigma, USA. 6-well, 24-well and 96-well cell culture plates were procured from Becton Dickinson, USA. Thiobarbituric acid (GR grade) was purchased from Loba Chemie, India. Malondialdehyde (MDA), lactate dehydrogenase (LDH), glutathione (GSH), superoxide dismutase (SOD) estimation kits were purchased from Accurex Biomedical Pvt. Ltd, India. Creatine kinase myocytes B (CK-MB) kit was purchased from Coral Biosystems, India. Acetone, acetonitrile and methanol (HPLC grade) were purchased from Merck, India. Ultra-pure deionized water (LaboStar™ ultrapure water Systems, Germany) was used for all the experiments. All other reagents used were of analytical grade and purchased from local suppliers unless mentioned.

Preparation of Dox-LCNPs

Dox-LCNPs were prepared by hydrotrope method (21). Briefly, Dox was dissolved in minimal quantity of water (250 µl) and diluted with ethanol (300 µl) containing phytantriol (100 mg). The resulting isotropic solution was added dropwise into the surfactant solution (10 ml) at stirring 2,000 rpm for 12 h. Ethanol diffusion followed by evaporation resulted in formation of Dox-LCNPs. Further, the resultant LCNPs were subjected to probe sonication at 30% amplitude for 10 s and the system was equilibrated by stirring at 500 rpm for 2 h. Finally, free Dox and surfactant were removed from

the formulation by dialysis (MW 15 kD, Sigma USA) against deionized water for 20 min at 250 rpm.

Optimization of Formulation Components and Process Variables

Exhaustive optimization of formulation components viz. ethanol concentration, type and concentration of stabilizer and % Dox loading and sonication time were carried out for preparation of Dox-LCNPs. The optimum parameters were selected on the basis of quality attributes (particle size, size distribution, zeta potential and encapsulation efficiency) of prepared Dox-LCNPs. During optimization, certain other minor experimental parameters like amount of lipid added (1% w/w with respect to dispersion), stirring speed, time and final volume of dispersion (10 ml) were kept constant.

Optimization of Ethanol Concentration

Various concentrations of ethanol (0.1–0.4% w/v) were tried for the preparation of Dox-LCNPs while keeping constant concentration of Dox (0.01% w/v) and Pluronic® F-108 (0.5% w/v) with respect to dispersion volume.

Optimization of Type of Stabilizer

Surfactant screening was conducted by preparing the Dox-LCNPs in presence of 0.5% w/v concentration of various types of Pluronic® surfactants (F-127, F-108, F-87 and F-68). The best stabilizer was implemented for further studies.

Optimization of Stabilizer Concentration

Various concentrations of Pluronic® F-127 (0.05–0.07% w/v with respect to dispersion volume) were evaluated in the preparation of Dox-LCNPs. The suitable concentration of surfactant was utilized for further optimizations.

Optimization of Drug Loading

Dox-LCNPs were prepared at various drug loading 10.0, 15.0, 17.5 and 20.0 (% w/w with respect to lipid) and their effect on formulation attributes was evaluated. The optimized drug loading was utilized for further studies.

Optimization of Sonication Time

Probe sonication was carried out to reduce the particle size as well as to improve the homogeneity of Dox-LCNPs. Sonication at amplitude of 30% was applied for 5, 10 and 20 s and its effect on particle size, PDI and entrapment efficiency was evaluated.

Lyophilization of Dox-LCNPs

The optimized dispersion of Dox-LCNPs was lyophilized (Vir Tis, Wizard 2.0, New York, USA freeze dryer) using a universal stepwise freeze-drying cycle developed and patented by our group (22). The type and concentration of cryoprotectant was selected from dextrose, trehalose, mannitol and sucrose based on its capabilities to retain the original quality attributes. Briefly, a volume of 0.5 ml of Dox-LCNPs along with cryoprotectant was filled in 5 ml glass vials and subjected to freeze drying. The freeze dried formulations were characterized for the appearance of cake, size, PDI, ease of redispersion and encapsulation efficiency after reconstitution (23).

Characterization of Dox-LCNPs

Particle Size and Zeta Potential

Dox-LCNPs were evaluated for their mean particle size, polydispersity index (PDI) and zeta potential by using Zeta Sizer (Nano ZS, Malvern Instruments, UK).

Hi-Resolution Transmission Electron Microscopy (HR-TEM)

The prepared formulations were further characterized for their shape and morphology by HR-TEM (FEI Tecnai G2, Fei Electron Optics, USA). Samples were stained with 1% w/v aqueous solution of phosphotungstic acid and processed as per the standard protocols reported earlier (21). The specimens were viewed under the microscope at an accelerating voltage of 100–200.0 kV.

Entrapment Efficiency

Dialysis method was employed to separation of free drug from LCNPs dispersion. Briefly, formulation was filled in the dialysis membrane (15 kD, Sigma, USA) and dialyzed against 50 ml water for 30 min at 500 rpm to separate unentrapped drug. The said procedure was optimized and validated in-house for complete separation of free Dox from formulation (see Supplementary Material, Figure S1). The formulation was then suitably diluted with ethanol and estimated (considered as direct method) using Shimadzu HPLC system with LC software coupled to RF-10AXL fluorescence detector using validated method with slight modification (5). The separation was achieved using a Symmetry® C18 (4.6× 150 mm, 5 µm; Waters, USA) analytical column fitted with Nuceasil C18 (Macherey-Nagel, Germany) guard column maintained at 30°C. Doxorubicin was isolated using a mobile phase consisting of acetonitrile and acetate buffer (20 mM, pH 4.5; 24:76%v/v) at flow rate of 1.0 mL/min. The injection volume was 20 µl and retention time of Dox was found to be

5.2 min. The Dox was analyzed by fluorimetric measurement at λ excitation of 480 nm and λ emission of 590 nm. Drug content in the dialyzing media (indirect method) was also estimated to check the mass balance, was found to >95% w/w in all cases.

Light Microscopy/Phase Behavior

The phase behavior (isotropic and anisotropic characteristics) of the lipid dispersion under influence of varied excipients at different concentrations was evaluated using a polarizing microscope (Nikon Eclipse LV 100, Japan) with and without crossed polarizer or differential interference contrast attached with Q imaging, 3.3 R TV camera. Briefly, the representative micron sized particles were prepared by dispersing 10% w/v lipid solution (200 µl, 55% v/v ethanol) in 0.5% surfactant solution (10 ml) at stirring speed of 750 rpm for 12 h. About 20 µl resultant thick dispersion was placed on a glass slide and examined under polarizing light microscopy at a magnification of 100× in order to study the existence of birefringence. The isotropic and anisotropic phases were identified according to classification established by Rosevear (24).

Small Angle X-ray Scattering (SAXS) Analysis

SAXS measurements were performed on a model SAXSess mc^2 (Anton Paar GmbH, USA) equipped with Kratky block-collimation system. The SAXS system comprised with a sealed-Cu tube X-ray generator (Philips, PW 1730/10) operating at 40 kV and 50 mA that generate Cu Kα radiation (wavelength 1.54 Å) which was calibrated with a silver behenate standard. The 2D CCD detector featured 2,084× 2,084 array with 24×24 μm^2 pixel size at a sample-detector distance of 311 mm was used to detect signals. Different samples were filled in capillary sample holder which was pre-equilibrated at 25°C for 30 min and exposed to X-ray beams for 90 min under vacuum. The temperature of the capillary was controlled by use of a Peltier system. The scattering files obtained after the analysis of samples were normalized for cosmic ray, detector background and water background by advanced data interpretation software (PCG). Further, the 2D images of scattering files were processed to the one-dimensional scattering function I(q), where q is the length of the scattering vector, defined by equation $q=(4\pi/\lambda)(\sin\theta/2)$, λ being the wavelength and θ the scattering angle. The cubic and hexagonal space groups of LCNPs were determined by the relative positions of the Bragg peaks displayed in the scattering curves, which correspond to the reflections on planes defined by their Miller indices (hkl). The validity of assigned miller indices was assessed by estimating the intercept of best fit curve obtained by plotting $(h^2+k^2+l^2)^{1/2}$ as a function of q ($Å^{-1}$). Moreover, the lattice parameter "a" was derived from the equation $a=4d/3\ (h^2+k^2)^{1/2}$ where the Bragg reflections are annotated using Miller indices hkl and d is the distance between the reflecting planes, defined by Bragg's law $d=2\pi/q$ (17).

Stability in Different GIT Fluids

Freeze-dried formulation was evaluated for its stability in simulated gastric fluids (SGF) and simulated intestinal fluids (SIF) in order to determine the robustness of formulation under different pH and enzymatic conditions. The SGF (pH 1.2) was composed of 0.2% NaCl, 0.7% pepsin and pH adjusted to 1.2 using 0.1 N HCl while SIF (pH 6.8) was composed of 0.685%w/v monobasic potassium phosphate, 1% w/v pancreatin and pH adjusted to 6.8 using 1% w/v NaOH. Reconstituted Dox-LCNPs (1 ml) was added to 20 ml simulated fluids and incubated for 2 h (in SGF) and 6 h (in SIF) in shaking water bath operated at 100 strokes per min at 37°C. The stability of Dox-LCNPs were evaluated in terms of particle size, PDI and % entrapment efficiency. Similarly, the stability of LCNPs was also studied after incubation in SGF for 2 h followed by re-incubation in SIF for 8 h (25).

Storage Stability

Storage stability of freeze dried formulation was tested at 25°C/55% RH for 6 months as per ICH guideline (26). Stability testing at said conditions was considered as "accelerated" owing to refrigeration requirement (2–8°C) for lyophilized Dox-LCNPs. The formulations were evaluated for particle size, PDI, zeta potential and % encapsulation efficiency after reconstitution.

In Vitro Release

The *in vitro* release of Dox from Dox-LCNPs was studied using dialysis membrane method. The Dox-LCNPs equivalent to 1 mg Dox were filled in dialysis bags (15 kD, Sigma USA) which was then suspended in 15 ml release medium (pH 7.4, 10 mM Tris buffer) and kept in shaking water bath (37.0± 1°C) operated at 100 strokes per min. Similar treatment was given to free Dox for comparative purpose. A 100 µl sample was withdrawn from release media and replenished with equal volume of fresh media. Concentration of Dox in the samples was measured by HPLC method (5) and the % cumulative release was calculated. Further, various release models were also implemented to predict mechanism of drug release (27).

Caco-2 Cell Culture Experiments

Cell Culture

Caco-2 cells (American Type Culture Collection) were grown in tissue culture flasks (25 cm^2) and maintained under 5%

CO_2 atmosphere at 37°C. The growth medium comprised of Minimum Eagle's culture medium (MEM), 20% fetal bovine serum (FBS), 100 U/ml penicillin and 100 µg/ml streptomycin and amphotericin B (PAA, Austria). The growth medium was changed on every alternate day until the confluency was reached. Once confluent, cells were harvested with 0.25% of Trypsin–EDTA solution (Sigma, USA) and either passaged or seeded in cell culture plates for further studies.

Qualitative Cell Uptake

Harvested Caco-2 were seeded in 6 well plate at a cell density of 3,00,000 cells/well and allowed to adhere overnight. The cells were then exposed to free Dox or free Dox with Cys A (10 µg/ml) or Dox-LCNPs at a dose equivalent to 1.0 µg/ml of free Dox and incubated for 4 h. Following the incubation period, medium was removed and cells were washed twice with the PBS, fixed with glutaraldehyde (2.5% v/v) and observed under the confocal laser scanning microscope (CLSM) (Olympus FV1000).

Quantitative Cell Uptake

Harvested Caco-2 cells were seeded in 24 well plate at cell density of 1×10^5 cells/well and allowed to adhere overnight. The cell were exposed to different concentrations of Dox formulations (a dose equivalent to 0.5 and 1 µg/ml of free Dox) and incubated for 0.5, 1, 2, 3, 4 and 6 h. After incubation, cells were washed 5 times with Hank's balanced salt solution (HBSS; PAA, Austria) to remove non-internalized drug/LCNPs and then lyzed with 400 µl of 0.1% v/v Triton X-100 solution in ethanol. The drug concentration in the cell lysates was estimated by HPLC as described previously (5).

MCF-7 Cell Culture Experiments

Cell Culture

MCF-7 (Human adenocarcinoma breast cancer cell line) was procured from National Centre for Cell Sciences, India. MCF-7 cells grown and maintained under 5% CO_2 at 37°C and 95% RH in 25 cm^2 tissue culture flasks were used for cell culture experiments. Cell culture medium MEM (Sigma, USA) was supplemented with 2.2% sodium bicarbonate, 1 mM sodium pyruvate, 10% fetal bovine serum (FBS), 100 U/ml penicillin and 100 µg/ml streptomycin and amphotericin B (Sigma, USA). The cells were harvested by 0.25% w/v trypsin-EDTA solution (Sigma, USA). once confluent and then sub-cultured in appropriate cell culture plates at a specified density for subsequent studies. Briefly, cells were seeded at a density of 50,000 cells/well in 6 well and 24 well culture plates (Costars, Corning Inc.) for analyzing qualitative and quantitative uptake, respectively.

Qualitative Cell Uptake

After the cells reached the confluency, the cell culture medium was removed and cells were washed with HBSS for three times. Free Dox and Dox-LCNPs (equivalent to 0.5 µg/ml of free Dox) were added to each plate and incubated for 4 h. Following the incubation period, medium was removed and cells were washed twice with the PBS and observed under the CLSM.

Quantitative Cell Uptake

The culture medium was replaced with fresh medium containing different concentrations of Dox formulations (1 and 2 µg/ml) and incubated for 1, 2, 3, 4, 6 and 8 h. After incubation, cells were processed as described in "Quantitative Cell Uptake on Caco-2 Cells".

Intracellular Trafficking

MCF-7 (1×105 cells/well) were seeded in 6-well culture plate and incubated overnight for cell attachment. The attached cells were incubated with Dox-LCNPs for 4 h (equivalent to 0.5 µg/ml of free Dox). After incubation, cells were washed twice with HBSS and re-incubated with 10 µg/ml vital dyes viz. Mitotracker® (Invitrogen-Life Technologies) and neutral red (Sigma, USA) for 15 min to label mitochondria and lysosomes, respectively. Subsequently, cells were fixed using 2.5% v/v glutaraldehyde solution, washed twice and permealized with Triton X-100. Nuclei of the permeabilized cells were then labeled with DAPI (10 ng/ml, 30 s). Labelled cells were then visualized under CLSM and fluorescence intensity of the dyes was measured. Various instrument operational parameters viz. pin hole size, electron gain, neutral density filters and background levels were set up before the confocal experiment and were not changed throughout the measurements. Line analysis, box analysis and % colocalization of images were assessed using data processing software of CLSM.

Cell Cytotoxicity

The cell cytotoxicity potential of free Dox and Dox-LCNPs was evaluated by seeding 1×10^4 cells/well in 96 cell culture plate and allowed to adhere overnight for cell attachment. The attached cells were incubated with different concentrations of free Dox/Dox-LCNPs for 24 h or 48 h and the cell viability was determined by SRB assay (28). Briefly, treated cells were stained with SRB (0.4% w/v in 1% acetic acid, 100 µl/well). The unbound dye was washed 5 times with 1% acetic acid and plates were air dried. Further,

100 μl Tris-buffer (0.01 M, pH 10.4) were added into each well and plates were gently shaken for 10 min on a mechanical shaker for complete dissolution of the adsorbed dye. The optical density (OD) was recorded using a 96 well plate reader (BioTek Instruments, Inc., USA) at 540 nm and % cell viability was calculated by following formula:

$$\%\ \text{cell viability} = 100 \times \frac{OD_{\text{test sample}} - OD_{\text{blank}}}{OD_{\text{Control}} - OD_{\text{blank}}}$$

In Vivo Pharmacokinetics

Animals and Dosing

Female Sprague Dawley (SD) rats of 220–250 g were supplied by the central animal facility, NIPER, India. All experimental protocols were duly approved by the Institutional Animal Ethics Committee, NIPER, India. The animals were housed as per standard housing conditions.

Animals were randomly distributed into two groups each containing 6 animals. Free Dox and Dox-LCNPs were administered to the overnight fasted animals by oral gavage at an equivalent drug dose of 10 mg/kg body weight. The blood samples (0.15–0.2 ml) were collected from the retro-orbital plexus under mild anesthesia into heparinized micro centrifuge tubes (containing 30 μl of 1000 IU heparin/ml of blood). Plasma was separated by centrifuging the blood samples at 5,000 rcf for 5 min at 15°C. To 100 μl plasma, 50 μl of 10 μg/ml internal standard (methyl paraben) was added followed by 500 μl methanol. The samples were vortexed for 15 min and centrifuged at 10,000 rpm for 15 min. The supernatants were separated and analyzed for drug content by validated RP-HPLC (Simadzu, Corp. Japan) using a fluorescence detector (RF-10AXL) (5).

The pharmacokinetic parameters of plasma concentration-time data were analyzed by one-compartmental model, using Kinetica software (Thermo scientific, USA). Various required pharmacokinetics parameters like total area under the curve $(AUC)_{0\text{-}\infty}$, time to reach the maximum plasma concentration (T_{max}) and peak plasma concentration (C_{max}) were determined. The relative bioavailability of formulations after oral administration was calculated as follows:

$$\text{Relative bioavailability} = \frac{AUC_{0-\infty}(\text{Formulation})}{AUC_{0-\infty}(\text{Drug solution})} \times 100$$

Tumor Growth Inhibition

Female Sprague Dawley rats of 180–200 g were treated with 7, 12-dimethylbenz[α]anthracene (DMBA) to induce breast cancer. Briefly, DMBA solution in soya bean oil was administered orally to female rats at a dose of 45 mg/kg body weight at weekly interval for three consecutive weeks (5,29). Tumor bearing animals were sorted after 10 weeks of the last dose of DMBA. The animals were randomly divided into different groups (each containing 6 animals) viz. control (oral administration of saline), Dox-LCNPs (*per oral*), Adriamycin® (*i.v.*), and LipoDox (*i.v.*). All the formulations were given at a dose equivalent to 5 mg/kg body weight of Dox (5). The tumor width (w) and length (l) were recorded with an electronic digital caliper and tumor size was calculated using the formula $(l \times w^2/2)$. Tumor volume was measured up to 30 days.

Dox-Induced Cardiotoxicity

Animals of the tumor growth inhibition study were humanely sacrificed after 30 days of Dox administration and blood was collected in heparinized appendroff tubes by cardiac puncture. The plasma was separated by centrifuging the blood samples at 5,000 rcf for 5 min and stored at −20°C until analyzed. Subsequently, whole hearts were also excised and representative part of each heart tissue was fixed in 10% (v/v) formalin solution and processed for histopathological procedures (paraffin embedded specimen were cut into 5 μm sections and stained with hematoxylin and eosin) (5). Remaining heart tissues were homogenized in 5 volume of ice cold PBS (pH 7.4) using homogenizer (Polytron PT 4000, Switzerland). The plasma samples were analyzed for levels of various enzymes such as CK-MB and LDH levels while heart homogenates were analyzed for MDA, GSH and superoxide dismutase (SOD) levels using the commercially available kits following the manufacturer's instructions.

Statistical Analysis

All *in vitro* and *in vivo* data are expressed as mean ± standard deviation (SD) and mean ± standard error of mean (SEM), respectively. Statistical analysis was performed with Sigma Stat (Version 2.03) using one-way ANOVA followed by Tukey–Kramer multiple comparison test. $p < 0.05$ was considered as statistically significant difference.

RESULTS

Effect of Formulation Components and Process Parameter on Dox-LCNPs

Optimization of Ethanol Concentration

As evident from Table I, a significant ($p < 0.05$) decrease in the particle size and PDI of Dox-LCNPs was observed with increase in ethanol concentration. The concentration beyond 0.3% *w/w* did not induce considerable changes in particle size and PDI,

Table I Effect of Ethanol on Particle Size, PDI, Zeta Potential, Phase Behavior and Entrapment Efficiency

Ethanol (% w/v)[a]	Size (nm)	PDI	Zeta potential (mV)	Phase behavior[b]	Entrapment efficiency (% w/w)[c]
0.10	Aggregated	–	–	Isotropic	76.24 ± 3.84
0.20	657.86 ± 34.87	0.39 ± 0.15	−21.25 ± 0.58	Isotropic	73.21 ± 2.25
0.25	354.54 ± 9.57	0.35 ± 0.08	−21.48 ± 0.67	Isotropic	71.43 ± 1.61
0.30	285.20 ± 6.37	0.26 ± 0.04	−21.75 ± 0.47	Isotropic	69.73 ± 1.76
0.40	278.41 ± 7.64	0.25 ± 0.06	−22.15 ± 0.35	Isotropic	61.42 ± 3.14

Values are expressed as mean ± S.D. ($n = 6$)

[a] 0.5% w/v (with respect to dispersion) Pluronic F-108 was taken as a stabilizer

[b] Based on observation under the polarizing microscope

[c] % w/w entrapment efficiency was determined for 5% drug loading with respect of lipid content

however, a significant ($p < 0.01$) decrease in entrapment efficiency of Dox was recorded. Hence, optimum concentration of ethanol 0.3% w/w was chosen for subsequent studies.

Optimization of Type and Concentration of Stabilizer

Insignificant change ($p > 0.05$) in the particle size of Dox-LCNPs was observed when different grades of Pluronic® were employed (Table II). However, entrapment efficiency was found to be significantly higher ($p < 0.01$) in case of Pluronic® F-127 as compared to the other grades of Pluronic®. Subsequently, the effect of concentration of Pluronic® F-127 was also evaluated. With increase in concentration (0.5–0.6% v/v), a significant ($p < 0.05$) decrease in the particle size along with improvement in the PDI was observed (Table III). However, further increase in the surfactant concentration did not show any appreciable change in the quality attributes. Thus, 0.6% w/v concentration was considered as optimum and used for further studies.

Optimization of Drug Loading

The evaluation of effect of drug loading revealed insignificant changes ($p > 0.05$) in entrapment efficiency and slight changes in particles size upon increasing the theoretical drug loading from 10 to 15% w/w (Table IV). Interestingly, at these loading ratios total amount of Dox was increased from 7.66 to 11.17 mg in the formulation and then became constant upon further increase in % drug loading. This suggested that maximum Dox loading could be achieved with 15% w/w theoretical drug loading. Therefore, the chosen optimum loading of Dox in the system was 15% *w/w*.

Optimization of Sonication Time

A significant reduction ($p < 0.05$) in particle size and improvement in the PDI was observed upon increasing the sonication time from 5 to 10 s at 30 amplitude. Further, increasing the sonication time (beyond 20 s) led to significant ($p < 0.001$) increase in the particle size along with significant ($p < 0.001$) decrease in entrapment efficiency of formulation (Table V). Thus, based on desired quality attributes (Particle size <300 nm and maximum entrapment efficiency) minimum sonication time (10 s) was considered to be an optimum value.

Lyophilization of Dox-LCNPs

Lyophilization of the prepared formulations was performed for stabilization purpose. Among the various cryoprotectants evaluated, 5% w/w mannitol yielded the promising results in retaining the original quality attributes of Dox-LCNPs

Table II Effect of Different Stabilizers on Particle Size, PDI, Zeta Potential, Phase Behavior and Entrapment Efficiency

Type of surfactant[a]	Size (nm)	PDI	Zeta potential (mV)	Entrapment efficiency (% w/w)[b]
Pluronic® F-68	276.43 ± 9.39	0.24 ± 0.01	−21.4 ± 0.12	64.65 ± 2.43
Pluronic® F-87	259.73 ± 7.61	0.23 ± 0.03	−22.45 ± 0.34	65.75 ± 1.94
Pluronic® F-108	285.20 ± 6.37	0.26 ± 0.04	−21.75 ± 0.47	69.73 ± 1.76
Pluronic® F-127	267.87 ± 7.24	0.28 ± 0.02	−21.46 ± 0.65	74.45 ± 2.17

[a] 0.5% w/v (with respect to dispersion) was taken as a stabilizer

[b] % w/w entrapment efficiency was determined for 10% drug loading with respect of lipid content

Table III Effect of Pluronic F-127 Concentration on Particle Size, PDI, Zeta Potential and Entrapment Efficiency

Surfactant (% w/v)	Size (nm)	PDI	Zeta potential (mV)	Entrapment efficiency (% w/w)[a]
0.50	267.87 ± 7.24	0.28 ± 0.02	−21.3 ± 0.82	74.45 ± 2.17
0.60	239.76 ± 7.71	0.22 ± 0.01	−21.63 ± 0.39	76.56 ± 2.57
0.70	241.43 ± 8.01	0.23 ± 0.03	−19.05 ± 0.67	75.4 ± 2.78

Values are expressed as mean ± S.D. ($n = 6$)

[a] % w/w entrapment efficiency was determined for 10% drug loading with respect of lipid content

(detailed data are not shown). Hence, mannitol was implemented for further studies which resulted in to formation of intact fluffy cake. Upon reconstitution, achieved within 2 min with gentle shaking, insignificant changes in the original quality attributes were observed with S_f/S_i ratio (ratio of the particle size after and before freeze drying) 1.09 (Table VI). Additionally, freeze dried Dox-LCNPs were also found to be stable following 6 months of accelerated stability testing.

Characterization of Dox-LCNPs

HR-TEM

The obtained HRTEM microphotograph of Dox-LCNPs showed discrete cubic geometry (Fig. 1a). The lipidic matrix of phytantriol along with the water channels were clearly observed upon further increasing the magnification (Fig. 1b). The observed particle size of Dox-LCNPs was found to be 214.12 ± 16.25 × 158.37 ± 11.45 nm (length × breadth; average of 50 particles). Notably, the observed dimensions were smaller than that obtained from the Zeta sizer (265.87 ± 5.54 nm).

Light Microscopy/Phase Behavior Studies

For microscopic studies, a representative micron sized Dox-liquid crystalline particulate formulation was prepared which showed a few aggregates in micrometer range when observed under light microscope (see Supplementary Material Fig. S2A, S2B). Additionally, both blank and drug loaded dispersion showed a dark background under polarized light which revealed their isotropic nature (21,30). This also suggested incorporation of amphiphilic Dox (up to 20% w/w/with respect to lipid) into the liquid crystalline phase did not alter their phase behavior.

SAXS Studies

SAXS analysis of Dox-LCNPs showed four distinct Bragg peaks (Fig. 2a) whose relative positions were found to be in ratios of √2:√4:√6:√8 which confirmed Pn3m type of cubic structure (31). Further, the miller indices (h,k,l) = (1, 1, 0), (2, 0, 0), (2, 1, 1), (2, 2, 0) for these peak were assigned (Fig. 2b). Based on miller indices, the lattice parameters and lattice constant for Dox-LCNPs were also calculated and found to be 127.17 Å and 11.22 Å, respectively. Similarly, presence of Pn3m type cubic structure in the plain LCNPs dispersion was also observed (data are not shown) as reported by other groups (15,32,33). The lattice constant for plain LCNPs were found to be (~6.95 Å) while it was (~11.22 Å) in the case of Dox-LCNPs.

Stability in Simulated Gastrointestinal Fluids

Stability of Dox-LCNPs in GIT fluids was performed and was found that LCNPs could retain their initial qualities attributes (insignificant changes in particles size and a slight decrease in entrapment efficiency) in the SGF as well as in SIF condition (Table VII). Additionally, presence of high amount of drug inside the carrier (65.71 ± 2.02% w/w) even after 8 h reflected drug retaining capability of LCNPs upon exposure to GIT environments.

In Vitro Release Study

An equilibrium dialysis membrane method was applied to determine the *in vitro* release profile of Dox from formulation (34). Free Dox solution was also utilized as a control, a complete release (97.13 ± 2.89%) within 2 h was found. But in case of Dox-LCNPs, a sustained biphasic release profile

Table IV Effect of Drug Loading on Particle Size, PDI, Zeta Potential and Entrapment Efficiency

Drug loading[a]	Size (nm)	PDI	Zeta potential (mV)	Entrapment efficiency (% w/w)	Amount of Dox (mg)	Phase behavior[b]
10	239.76 ± 7.71	0.22 ± 0.01	−21.63 ± 0.39	76.56 ± 2.57	7.656 ± 2.57	Isotropic
15	265.87 ± 5.54	0.22 ± 0.04	−20.23 ± 0.32	74.65 ± 1.76	11.19 ± 2.64	Isotropic
17.5	272.45 ± 8.35	0.24 ± 0.04	−21.42 ± 0.49	62.38 ± 1.87	10.91 ± 3.27	Isotropic
20	275.87 ± 7.81	0.25 ± 0.04	−18.98 ± 0.52	55.91 ± 2.76	11.82 ± 5.52	Isotropic

Values are expressed as mean ± S.D. ($n = 6$)

[a] % w/w with respect to lipid content

[b] Based on observation under the polarizing microscope

Table V Effect of Sonication Time on Particle Size, PDI, Zeta Potential and Entrapment Efficiency

Sonication time (Sec)	Size (nm)	PDI	Zeta potential (mV)	Entrapment efficiency (% w/w)
5	289.98 ± 8.98	0.27 ± 0.03	−21.33 ± 0.62	75.25 ± 2.16
10	265.87 ± 5.54	0.22 ± 0.04	−20.23 ± 0.32	74.65 ± 1.76
20	256.26 ± 4.32	0.23 ± 0.04	−19.87 ± 0.42	72.45 ± 2.34
30	386.84 ± 10.57	0.24 ± 0.05	−20.14 ± 0.51	65.17 ± 3.19

Values are expressed as mean ± S.D. ($n = 6$)

composed of a relatively faster release in initial 12 h (38.86 ± 2.15%) followed by a sustained release till 120 h (96.7 ± 2.1%) was observed (Fig. 3). In order to infer the mechanism of Dox release from LCNPs, the data of release studies were fitted in various kinetic models. It is inferred from Table VIII that Dox-LCNPs preferentially followed Hixson-Crowell and Korsmeyer Peppas (slope $n = 0.43$, suggesting fickian diffusion as mechanism of drug release).

Cell Culture Experiments

Caco-2 Cell Uptake

Figure 4a represents the confocal images of Caco-2 cells upon 4 h incubation with free Dox, free Dox with Cys A and Dox-LCNPs. The images show higher intracellular uptake of Dox-LCNPs as compared to both free Dox and free Dox with Cys A (a known P-gp inhibitor). Further, the quantitative uptake studies revealed alteration in steady state intracellular concentration of Dox in case of Dox-LCNPs and free Dox (alone or with Cys A) (Fig. 4a). The steady state concentration

Table VI Physicochemical Properties of Dox-LCNPs and Freeze Dried Dox-LCNPs

Parameters	Dox-LCNPs	Freeze dried Dox-LCNPs	
		Initial	After six months
Particle size (nm)	265.87 ± 5.54	289.5 ± 6.74	274.84 ± 8.64
PDI	0.22 ± 0.04	0.23 ± 0.03	0.24 ± 0.05
Zeta potential	−20.23 ± 0.32	−20.34 ± 0.37	−20.14 ± 0.47
Entrapment efficiency (% w/w)	74.65 ± 1.76	73.89 ± 1.97	72.54 ± 2.14
Physical appearance		Intact fluffy cake	
Ratio (S_f/S_i)		1.09	
Reconstitution time		< 100 s	< 100 s

Values are expressed as mean ± SD ($n = 6$); Reconstitution was performed in 0.5 ml of the vehicle followed by gentle agitation

in case of co-incubation of free Dox with Cys A was found to be 64.63 ± 5.79 ng/ml at 6 h in contrast to that of free Dox (42.81 ± 3.14 ng/ml at 6 h). Interestingly, the same was found to be higher (731.04 ± 38.51 ng/ml) and achieved in lesser time (only 2 h) in case of Dox-LCNPs at 1.0 μg/ml (Fig. 4c). The values suggest attainment of ~17.08- and 11.31-fold higher concentration of Dox which was achieved in one third time in case of Dox-LCNPs as compared to free Dox and free Dox + CysA respectively. Furthermore, cells viability was also found to be >90% in all the cases indicative of absence of any toxicity to Caco-2 cells at tested concentration (1.0 μg/ml). The studies at higher concentration of Dox-LCNPs and blank LNCPs were also performed but dramatic decrease in the cell viability was observed in both the formulations suggesting interaction of LNCPs with cells. Hence, a systematic study design was employed for evaluating the effect of LNCPs on cells. The results revealed concentration dependent alteration in the cells morphology (Fig. 4b) in case of LCNPs. Notably, the interaction was found to be concentration dependent with threshold concentration of LNCPs at 80–100 μg/ml of lipid. The cell viability was found to be ~40% at 100 μg/ml in contrast >90% below 80 μg/ml. In contrast, no such alteration in the cell morphology was observed in case of formulation excipients (either lipid or surfactant) at all tested concentration suggesting excipients has no detrimental effects on Caco-2 cells.

MCF-7 Uptake and Intra Cellular Trafficking

Qualitative uptake of Dox-formulation in MCF-7 cells were also carried out to demonstrate their uptake efficiency. Confocal images of MCF-7 cells upon 4 h incubation with free Dox and Dox-LCNPs have been displayed in Fig. 5a. The images demonstrate higher intracellular uptake of Dox by Dox-LCNPs as compared to free Dox. Further, concentration and time dependent cellular uptake of Dox in MCF-7 cells by Dox formulations was carried out to infer details of the uptake kinetic (Fig. 5a and b). Significantly higher ($p < 0.001$) and rapid steady state concentration of Dox was achieved in case of Dox-LCNPs (1314.8 ± 71.5 ng/ml at 3 h) in contrast to free Dox (287.65 ± 6.35 ng/ml at 6 h) at 2.0 μg/ml of Dox concentration (Fig. 5b). The values suggest ~4.57-fold increase in the concentration of Dox in 50% lesser time by Dox-LCNPs as compared to free Dox. The cell cytotoxicity experiments revealed >90% of cell viability in all the cases.

Further, the intracellular co-localization of Dox-LCNPs and nuclear-specific DAPI dyes was assessed by qualitative (line analysis and box analysis) and quantitative (scatter plot analysis) tools. Dox-LCNPs showed marked co-localization with DAPI suggesting higher nuclear co-localization which was further confirmed by line analysis (Fig. 6). The observed co-localization was further analyzed using scatter plots which

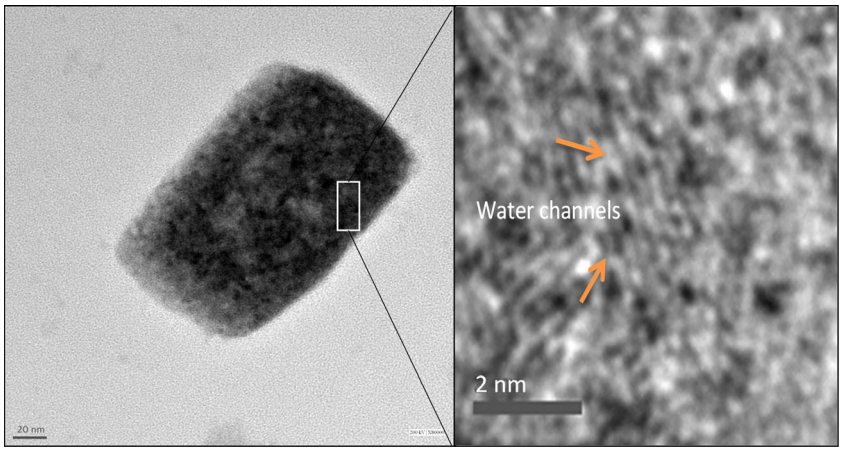

Fig. 1 TEM photograph of (**a**) Dox-LCNPs at 200 KV × 80,000 magnification and (**b**) part of Dox-LCNPs at 200 KV × 2,00,000 magnification. The *arrow* demonstrating the evidence of water channels.

showed ~76% of co-localization with nucleus after 4 h of incubation (Fig. 6e). In order to further determine the intracellular organelles localization of Dox-LCNPs, inherent red fluorescence of Dox was not found to be suitable due to overlapping of its fluorescence spectra with other red organelles dyes (Mitotracker® and NR). Thus, to avoid these artifacts, coumarin-6 loaded LCNPs were utilized for mitochondrial and lysosomal localization. As evident from line, scattered and box plot analyses (see Supplementary Material Fig. S3), the LCNPs was showed poor co-localization with mitochondria and lysosomes.

Cell Cytotoxicity Studies

The concentration and time dependent cytotoxicity against the MCF-7 cells was observed in case of both free Dox and Dox-LCNPs. However, Dox-LCNPs showed relatively higher cytotoxicity (69.65 ±3.98% growth inhibition) as compared to free Dox (35.46 ±3.57% growth inhibition) after 48 h upon incubation at 2 µg/ml concentration (Fig. 7). The value of IC_{50} for Dox-LCNPs was found to be ~1.75 µg/ml and ~0.25 µg/ml following 24 h and 48 h incubation, respectively which was 3.12- and 16.23-fold lower as compared to free Dox (Fig. 7). The cell cytotoxicity of the blank formulation was also evaluated which showed >90% cell viability revealing its biocompatibility (Fig. 7).

In Vivo Studies

Pharmacokinetic Studies

The *in vivo* pharmacokinetic studies revealed significantly higher ($p < 0.001$) C_{max} in case of Dox-LCNPs in contrast to that of free Dox, showing about 5.34-fold appreciation (Table IX). Moreover, sustained plasma profile of Dox upto 48 h was observed in case of LCNPs as compared to free Dox which demonstrated upto 12 h only (Fig. 8). The mean $AUC_{0-\infty}$ for Dox-LCNPs was 5974.19±874.65 ng/ml.h which indicated 17.74-fold higher relative bioavailability of Dox-LCNPs than that of free Dox (Table IX).

Tumor Growth Inhibition

Significant restriction in the tumor growth was observed in all cases except control which showed increase in tumor volume upto 158.66% in 30 days (Fig. 9). The reduction in tumor volume was of significantly higher and extended up to 22 days in case of orally administered Dox-LCNPs in contrast to Adriamycin® (*i.v.*) which showed reduction up to 10 days only. After 30 days, % residual tumor burden in case of *per oral* Dox-LCNPs (~58%) was markedly lower than that of clinical formulation of Adriamycin® *i.v.* (~69%). In contrast, lowest residual tumor burden was found in case of LipoDox®

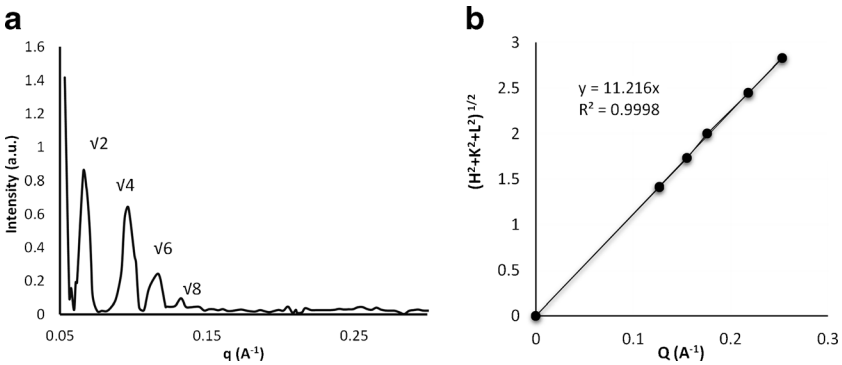

Fig. 2 Small angle X-ray analysis of Dox-LCNPs shows (**a**) diffraction peaks with their Miller indices and (**b**) validation of assigned Miller indices.

Table VII Stability Studies of Dox-LCNPs in Various GIT Fluids

Type of fluids	Size (nm)		PDI		Zeta potential (mV)		Entrapment efficiency (% w/w)	
	Initial	Final	Initial	Final	Initial	Final	Initial	Final
SGF (2 h)	289.5 ± 6.74	282.71 ± 6.15	0.23 ± 0.03	0.23 ± 0.03	−20.34 ± 0.37	−20.41 ± 0.32	74.65 ± 1.76	71.73 ± 1.39
SIF (6 h)		271.23 ± 7.81		0.21 ± 0.03		−20.61 ± 0.41		66.46 ± 1.58
SGF (2 h) + SIF (4 h)		278.56 ± 6.54		0.22 ± 0.06		−21.04 ± 0.38		65.71 ± 2.02

Values are expressed as mean ± SD ($n = 6$)

(*i.v.*), reducing up to ~85%. Interestingly, upon comparing residual tumor burden at 20 days, insignificant difference between *per oral* Dox-LCNPs (53.5 ±6.1%) and *i.v.* LipoDox® (46.8 ±8.4%) was observed (Supplementary Material Fig. S4). The results cumulatively suggest comparable therapeutic efficacy till 20 days to that of LipoDox® (*i.v.*) followed by which the efficacy of Dox-LCNPs diminishes demanding multiple dose and/or dose adjustments.

Dox-Induced Cardiotoxicity

Figure 10 depicts the levels of various cardiotoxicity markers estimated in plasma and heart homogenate after treatment with different formulations. The animals treated with Adriamycin® (*i.v*) and LipoDox® (*i.v*) posed significantly higher levels of CK-MB in plasma (Fig. 10a) as compared to control. Additionally, LDH levels and MDA in heart homogenates (Fig. 10b and c) were also significantly higher as compared to control. Simultaneously, the levels of GSH and SOD in heart homogenates were significantly ($p < 0.001$) decreased in case of Adriamycin® (*i.v.*) and LipoDox® (*i.v.*) as compared to that of control. The findings were further supported by histopathological examination, which revealed loss in structural integrity and myofibrillar architecture in heart tissue of animals treated with Adriamycin® (*i.v*) (Fig. 11b). Interestingly, no marked changes in cardiac tissue were observed in case of Dox-LCNPs (*per oral*) as compared to that of control (Fig. 11c). Similarly, significant changes ($p < 0.05$) in the levels of all cardiotoxicity markers were observed in case of Dox-LCNPs in comparison to that of clinical formulations suggesting marked reduction in the cardiotoxicity (Fig. 10).

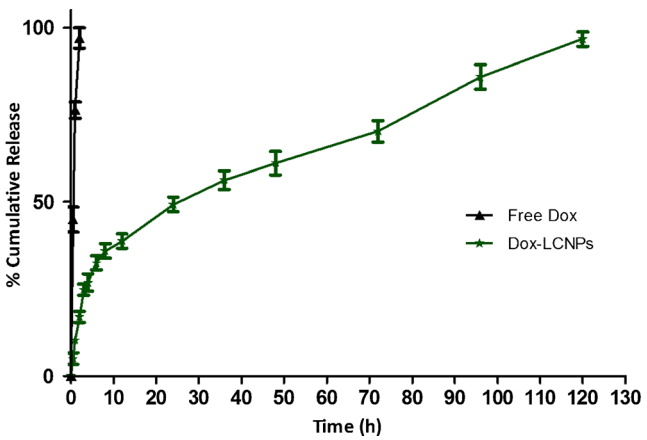

Fig. 3 *In vitro* release profile of free Dox and Dox-LCNPs.

DISCUSSION

Dilution through hydrotrope method was implemented for preparation of drug-loaded LCNPs (35,36). This method required low energy input to produce small, uniform size and stable particles in contrast to conventional high-shear and high-pressure dispersion methods (21,36). The ethanol was employed as a hydrotrope because it preferentially solubilizes the lipid and prevents its aggregation during pre-mixing with aqueous solution of Dox and surfactant solution. It also presumes a homogeneous nucleation process (driven by concentration of hydrotrope) during formation of LCNPs. The concentration below 0.25% w/w led to formation of LCNPs with higher particle size (>300 nm) and PDI (>0.3) owing to very high viscosity of lipidic phase. In contrast, the higher concentration resulted into rapid diffusion of lipidic phase and ultimately resulted into lower entrapment efficiencies (Table I). Hence, the initial concentration of hydrotrope and the viscosity of the organic phase play a critical role in the formation of LCNPs. Once nucleation starts the discrete LCNPs are usually stabilized by suitable

Table VIII Drug Release Parameter (Correlation Coefficient) Dox-LCNPs After Fitting in Various Release Models

Curve fitting model	Correlation coefficient
Zero order	0.846
First order	0.951
Higuchi	0.962
Hixon Crowell root	0.975
Korsmeyer Peppas	0.977, $n = 0.43$

Values are expressed as mean ± S.D. ($n = 6$)

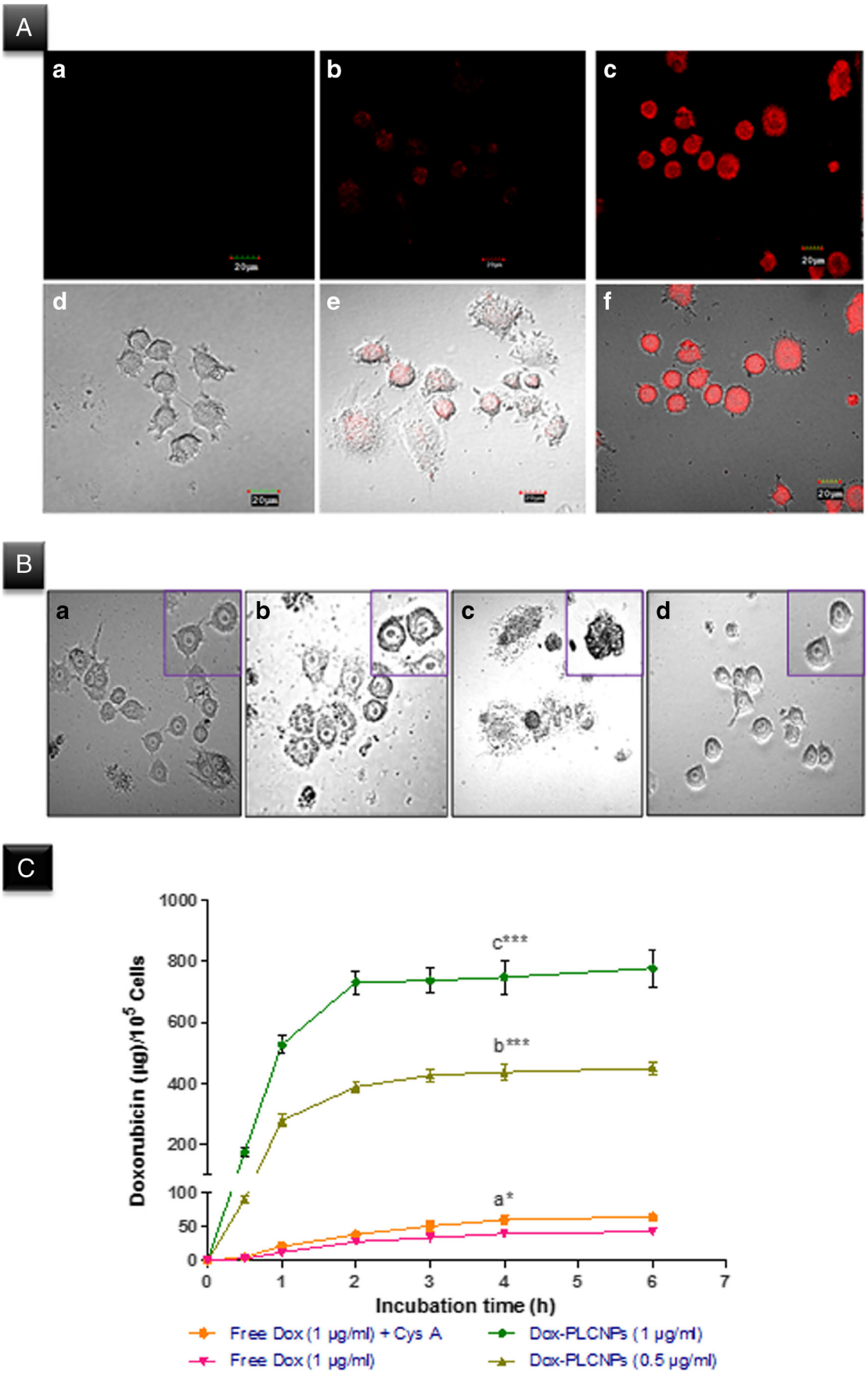
A
a
b
c
d
e
f
B
a
b
c
d
C
Doxorubicin (μg)/10^5 Cells
1000
800
600
400
200
100
50
0
c***
b***
a*
0
1
2
3
4
5
6
7
Incubation time (h)
Free Dox (1 μg/ml) + Cys A
Free Dox (1 μg/ml)
Dox-PLCNPs (1 μg/ml)
Dox-PLCNPs (0.5 μg/ml)

◀ **Fig. 4** Uptake of formulation in Caco-2 cells (**A**) CLSM images of the cells after 4 h incubation with (**a**) free Dox (1 μg/ml), (**b**) free Dox (1 μg/ml) + CysA (10 μg/ml), (**c**) Dox-LCNPs (equivalent to 1 μg/ml of free Dox), (**d**, **e**, **f**) overlay image of corresponding fluoresces and differential interference contrast (DIC) image of Caco-2 cells; (**B**) Differential interference contrast (DIC) images of cells, 20×, showing alteration in cell morphology after 3 h incubation with blank LCNPs at concentration of (**a**) 50 μg/ml, (**b**) 100 μg/ml, (**c**) 200 μg/ml, (**d**) control cells. The inset image shows enlarge view of representative cells. (**C**) shows concentration and time dependent quantitative uptake of Dox-formulation in Caco-2 cells; ***$p = 0.001$, *$p = 0.05$; (**a**) *vs*. free Dox (1 μg/nl), (**b**) free Dox (1 μg/ml) + CysA, (**c**) *vs*. Dox-LCNPs (0.5 μg/ml). Each data point is represented as the mean ± SD ($n = 6$).

surfactants. The present study encompasses high molecular weight nonionic triblock copolymers (Pluronic® series) considering their capability to preferentially adsorb on the surface of LCNPs and avoid unwanted mesophase structure transitions in contrast to low molecular weight copolymers which have tendency to affect the interior phase of liquid crystals (37). Among the tested surfactants from the series, maximum entrapment efficiency was observed in case of Pluronic® F-127 which could be attributed to its high lipophilic and large molecular weight resulting into lower

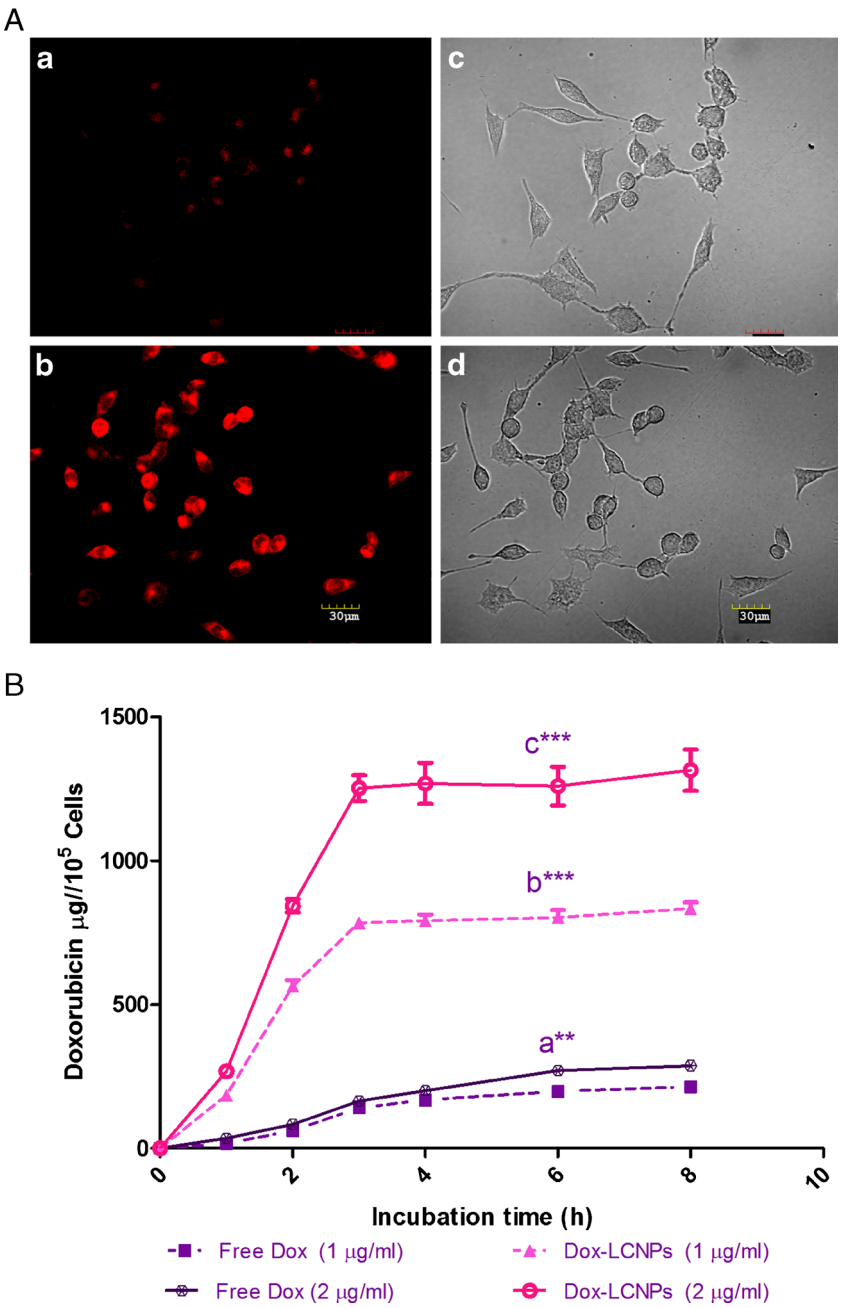

Fig. 5 Uptake of Dox in MCF-7 cells (**A**) CLSM images of the cells after 4 h incubation with (**a**) free Dox (1 μg/ml), (**b**) Dox-LCNPs (equivalent to 1 μg/ml of free Dox), (**c**, **d**) corresponding differential interference contrast (DIC) image of MCF-7 cells treated with free Dox and Dox-LCNPs respectively; (**B**) shows concentration and time dependent quantitative uptake of Dox formulation in MCF-7 cells, ***$p = 0.001$, **$p = 0.01$; (*a*) *vs*. free Dox (1 μg/nl), (*b*) free Dox (2 μg/ml), (*c*) *vs*. Dox-LCNPs (1 μg/ml); Each data point is represented as the mean ± SD ($n = 6$).

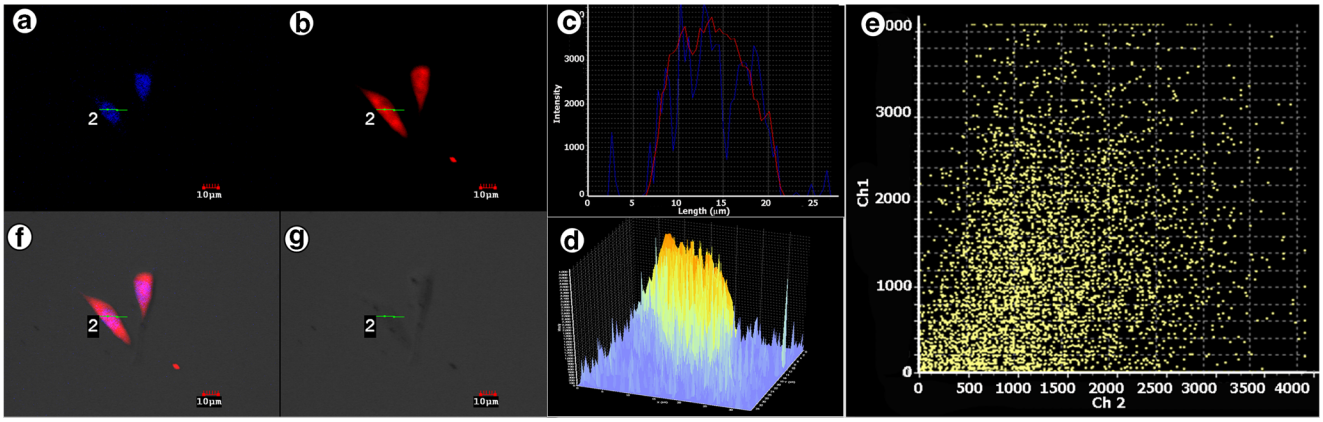

Fig. 6 Intracellular co-localization of (**a**) Dox-LCNPs with (**b**) DAPI-stained nucleus of MCF-7 cells. Line analysis plot (**c**) and box analysis (**d**) shows DAPI-Dox interaction while scatter plots (**e**) shows % co-localization of Dox-LCNPs co-localizing with DAPI. (**g**) Overlay image of (**a**, **b** and **f**) (DIC image).

hydrophilic-lipophilic balance value (Table II) (38). The selection of lipophilic surfactant i.e. Pluronic® F-127 also contrasts to the hydrophilic nature of Dox and hence assists in maximizing the entrapment efficiency due to reduced leaching of drug during formation of LCNPs. Similar relation between drug solubility in surfactant and entrapment efficiency of the carrier system has also been reported earlier (39). Further, the concentration of the surfactant was found to directly correlate with the PDI revealing the stabilization potential of surfactant in the formation of LCNPs (Table III). The optimized formulation was then subjected to effect of drug loading and saturation of drug-space in LCNPs was observed above 15% w/w (Table IV). Furthermore, effect of sonication was also employed for its influence on particle size and entrapment efficiency and was found that upon imparting higher energy (>10 s at 30 amplitude), acceleration in the kinetic energy of Dox-LNCPs increased drastically which resulted in destabilization of surfactant assisted steric barrier on the LCNPs and ultimately caused aggregation of particles (Table V). The final formulation was then lyophilized using universal stepwise freeze drying cycle developed and patented by our group (22). Implementation of 5% w/v mannitol in the lyophilization of Dox-LCNPs maintained all original quality attributes of formulations such as particle size, PDI and encapsulation efficiency and also demonstrated 6 months of accelerated stability (Table VI).

Morphological analysis of the developed formulation by HR-TEM revealed their cubic morphology with evidence of water channels within the structure which dried during sample preparation (Fig. 1). This could be the probable reason for slightly lower particle size observed with TEM as compared to that of Zeta Sizer (40). Additionally, the discrepancies in the particle size could also be attributed to the differences in the operating principle of analytical techniques, transmission of electron beam under the high vacuum in former case while measurement of hydrodynamic volume at normal room temperature in later case (41). The crystallinity was further established using SAXS (42,43). The spectral pattern of Dox-LCNPs depicted four diffraction peaks with relative ratio of

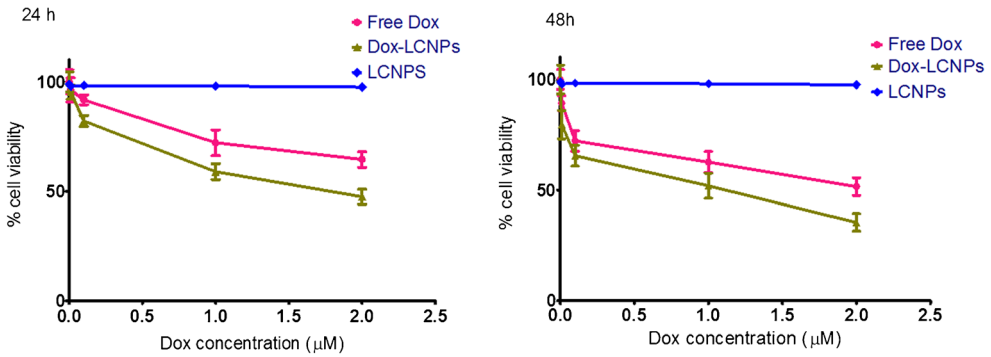

Fig. 7 Concentration- and time-dependent cell viability of MCF-7 cells upon treatment with Dox formulations. Table shows IC_{50} (μg/ml) value of Dox formulation at different incubation time. Each data point were expressed as mean ± SD ($n = 6$).

IC_{50} (μg/ml) values of Dox-formulations

Formulations	24 h	48 h
Free Dox	5.54	4.13
Dox-LCNPs	1.75	0.25

Table IX Pharmacokinetic Parameters After Oral Administration of Dox Formulations

Parameters	Free Dox	Dox-LCNPs
C_{max} (ng/ml)	35.58 ± 4.43	190.06 ± 30.89
T_{max} (h)	4	2
AUC_{0-t} (ng/ml*h)	322.09 ± 34.25	4022.54 ± 489.42
$AUC_{0-\infty}$ (ng/ml*h)	337.27 ± 59.75	5974.19 ± 874.65

Values are expressed as mean ± SEM ($n = 6$)

√2:√4:√6:√8 suggestive of Pn3m type cubic structure of developed LCNPs (Fig. 2a). Furthermore, assignment of crystallographic space groups i.e. miller indices as (hkl) = (1, 1, 0), (2, 0, 0), (2, 1, 1), (2, 2, 0) for Dox-LCNPs were considered to be valid (Fig. 2b) because points of the graph demonstrated a linear trend line (r^2 values >0.99) which intercepts at origin (0,0). The increased value of lattice parameter (~5 Å) in Dox-LCNPs in comparison to blank LCNPs reflected that hydration of LCNPs (or widening of the water channels) due to presence of Dox either in the aqueous domain or at the interface of the polar head group and apolar tail of the lipid. Such type of interactions have been reported for both hydrophilic and lipophilic drugs (21,44,45). The observed structural information (cubic) from SAXS studies also corroborates with the results of polarizing microscopy (isotropic structure; see Supplementary Material Fig. S1).

In vitro stability studies in simulated gastrointestinal fluids revealed robustness of formulation in GIT fluids because of insignificant change ($p > 0.05$) in particle size, PDI and zeta potential (Table VII). The entrapment efficiency of Dox in the formulation was also maintained due to characteristic feature of LCNPs which include chemical and structural stability of phytantriol based systems (17,46), surfactant assisted steric stabilization of the nanoparticles and sustained release characteristic of LCNPs limiting exposure of drug to exterior harsh environments thus minimizing drug degradation in GIT.

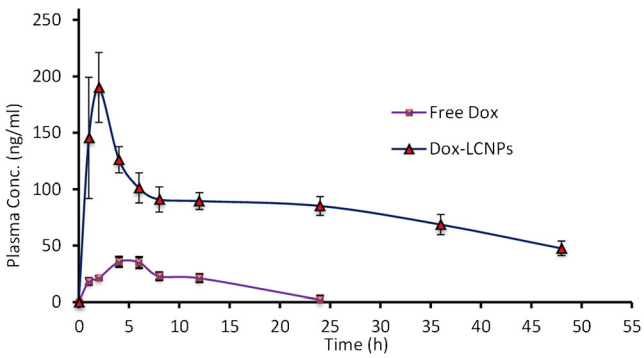

Fig. 8 Plasma concentration-time profiles of free Dox and Dox-LCNPs after oral administration to SD rats at 10 mg/kg dose. Each data points are expressed as mean ± SEM ($n = 6$).

In vitro drug release studies of Dox-LCNPs revealed sustained and biphasic release profile (Fig. 3). The drug release from Dox-LCNPs preferentially follows that Hixson-Crowell and Korsmeyer Peppas models indicating that the release mechanism may be by diffusion, swelling of matrix followed by erosion of the lipid matrix. Similar type of the release mechanism was also previously reported for lipidic system (25). Furthermore, presence of crystalline structure also imparts rigidity to the system hence making it like a matrix system hence these system also followed the Higuchi model (Table VIII). Broadly, it is postulated that presence of drug at the surface along with its higher concentration in the system at initial hour was responsible for rapid release. Further, time dependent continuous increase in diffusion path length for Dox, which was tortuous in nature, might also have played a role after certain time and might be responsible for a sustained release of Dox (47).

Complementary to drug release studies, *in vitro* Caco-2 uptake experiments further revealed significantly higher uptake of Dox-LCNPs as compared to free Dox at all tested concentrations (Fig. 4). The uptake was even higher as compared to that of Dox co-incubated with a known P-gp inhibitor, CysA, suggesting the involvement of other uptake mechanisms in case of Dox-LCNPs. The said observation could be correlated with membrane modifying (fluidity or fusion) properties of LCNPs as reported earlier (21,48,49) along with other uptake mechanisms such as clathrin and caveolae/lipid raft-mediated endocytosis (48) and transportation across the cells by long chain fatty acid transporters (50). Some reports also demonstrated complications associated with cell culture studies (49) owing to dominating membrane modifying properties of LCNPs. To address this, concentration dependent alterations in the morphology was evaluated for blank LCNPs which revealed existence of threshold concentration (~80–100 μg/ml) beyond which membrane modifying potential resulted in detrimental effects on cells (~40% cells viability at 100 μg/ml). Interestingly, the cell viability was found to be >90% in cases below threshold concentration (<80 μg/ml). Concomitantly, the CLSM studies revealed some morphological changes in the cell membrane (altered membrane integrity), referred to as "virtual paths" during uptake phase of LCNPs (Fig. 4b). These morphological changes were found to be reversible in nature when measured as a function of time and normal morphology regained within 12 h (data not shown). Thus, based on these observations a mechanism of uptake via formation of some reversible "virtual pathways" in the cell membrane might also possible along with above mentioned uptake mechanisms.

In vitro cell cytotoxicity potential of Dox-formulations was also evaluated against MCF-7 cells. Results revealed time dependent increase in the cytotoxicity in case of both free Dox and Dox-LCNPs. However, the magnitude of

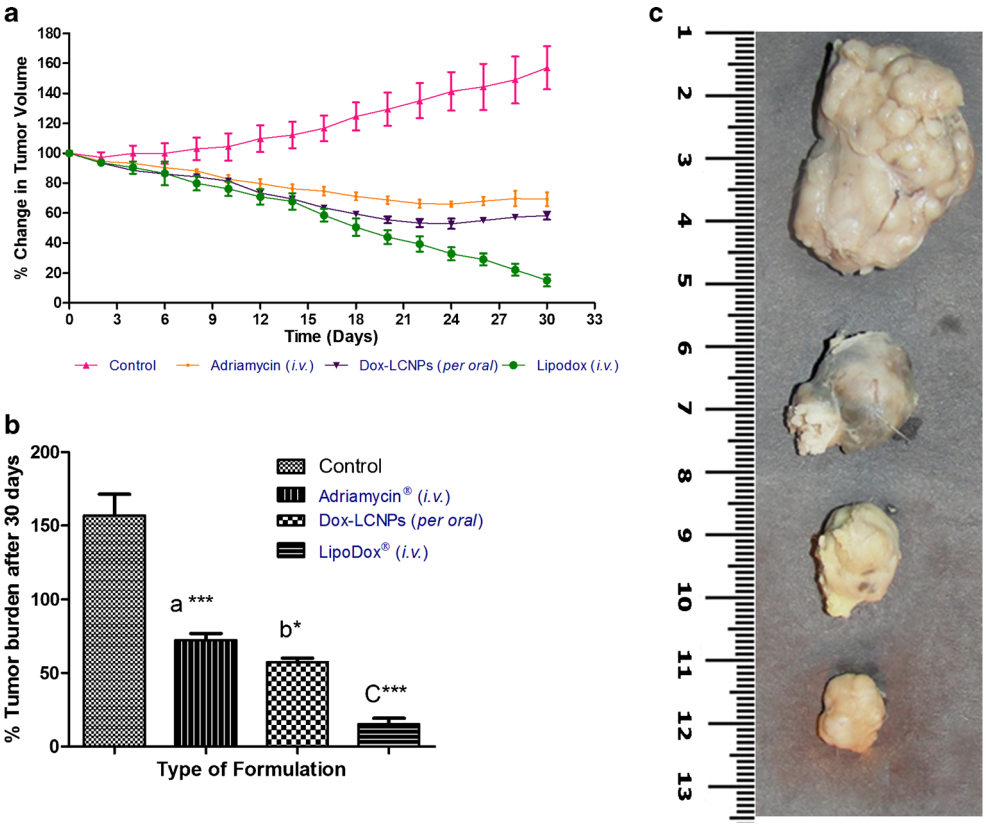

Fig. 9 *In vivo* antitumor efficacy of Dox-formulations in DMBA-induced tumor bearing female SD rats: (**a**) time-dependent tumor progression in animal, (**b**) tumor burden in animals after 30 days, (**c**) photographs of representative excised tumors from different treatment groups after 30 days. Mean tumor volume was taken as 100% at the start of drug treatment and tumor progression monitored until the end of the study. ***$p = 0.001$, *$p = 0.05$; (*a*) *vs*. Control (vehicle treated), (*b*) *vs*. Adriamycin® (i.v.), (*c*) *vs*. Dox-LCNPs. Each data point is represented as the mean ± SEM ($n = 6$).

cytotoxicity was significantly high ($p < 0.001$) in case of Dox-LCNPs which showed 3.12 and 16.23-fold decrease in IC_{50} value following 24 h and 48 h of incubation, respectively (Fig. 7). The possible reasons for such higher cytotoxic potential of Dox-LCNPs can be attributed to their rapid and higher internalization as compared to free Dox. Interestingly, the observed cytotoxic potential was higher than previously prepared Dox-PLGA-NPs (5). This could be correlated with the principal advantages associated with lipid based drug delivery systems which include multiple cellular internalization mechanisms and relatively higher drug release characteristics as compared to that of polymeric nanocarriers (51). Moreover, Dox-LCNPs demonstrated translocating capabilities to the site of drug action, i.e. nucleus (Figs. 5 and 6). As far as existing literature is concern, this is the first report which revealed that LCNPs prepared by phytantriol and stabilized by Pluronic® F-127 have tendency to localize near the vicinity of nucleus. Although, it has been reported that certain surfactants like Pluronic® and polyvinyl alcohol or surface modification of lipid matrix either by charge modifier like chitosan or nuclear targeting ligand, can facilitate cellular entry and nuclear transport of bioactives (5,39,52,53). However, none of the reports have shown nuclear co-localization of the said combination. Although, detailed study is warranted to explore the reason of nuclear colocalization of present LNCPs.

Results of pharmacokinetic studies further exhibited deliverability potential of Dox-LCNPs with 17.74-fold increase in the oral bioavailability in comparison to free Dox. This is one of the highest bioavailability achieved as compared to other reported carrier system exploited till date (1,7,8,54). Notably the plasma levels were also maintained for 48 h in case of Dox-LCNPs which could be attributed to the superior encapsulation and sustained release characteristic of LCNPs. Additionally, the LCNPs and their secondary structures are bioadhesive which increases the opportunities of close contact of drug loaded LNCPs with endothelial cell membrane and could overcome "unstirred water layer" barrier (55). Subsequently, lipid-mixing, membrane-fusing and formation of "virtual pathway" may also help in enhancing bioavailability of Dox (Figs. 8 and 4b). However, one can also evaluate the potential of crystallinity of LCNPs in making the system eligible for intestinal epithelial M cells uptake classically applicable to particulate carrier.

The promising pharmacokinetic profile of Dox-LCNPs inspired for evaluating its *in vivo* antitumor tumor efficacy in DMBA induced breast cancer model, already established in our lab (5,8,25,39,51). Tumor bearing rats treated with Dox-LCNPs showed a significant reduction ($p < 0.001$) in tumor volume in comparison to Adriamycin (*i.v.*) (Fig. 9). The relatively higher tumor restriction capability of Dox-LCNPs could be attributed to longer circulation half-life vis-a-vis passive targeting to tumor via enhanced permeation and

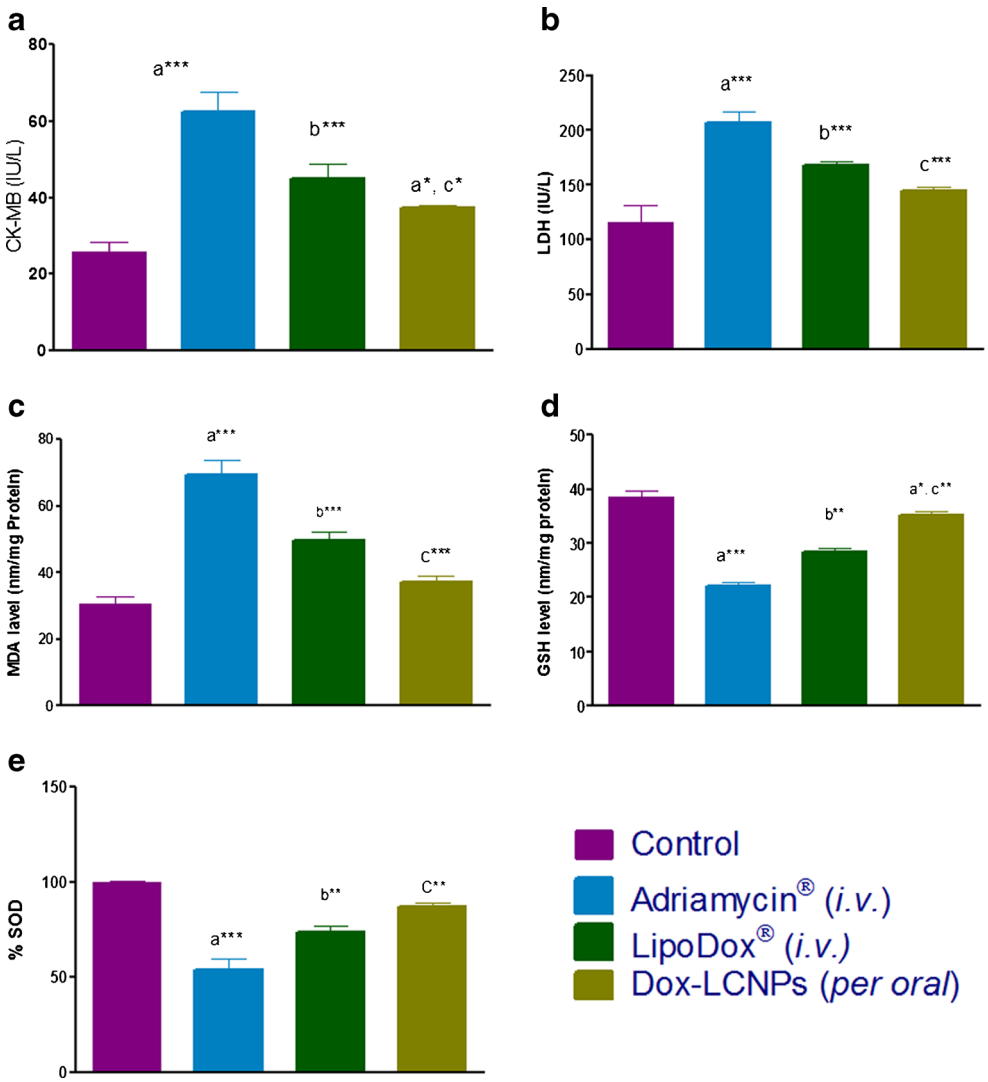

Fig. 10 Levels of various biochemical parameters in Plasma (**a**) CK-MB, (**b**) LDH and in heart homogenate (**c**) Lipid peroxidation products (MDA), (**d**) GSH levels and (**e**) % SOD, after 30 days of treatment with different formulations. ***$p < 0.001$, **$p < 0.01$, *$p < 0.05$; (*a*) *vs*. control, (*b*) *vs*. Adriamycin® (i.v.), (*c*) *vs*. LipoDox® (i.v.).

retention effect (EPR) as compared to that of free Dox. The results are in line with previous studies (5,30,39,56). Interestingly, the observed responses were found to be higher than our previously reported polymeric formulation of Dox (5). However, the residual tumor burden after 30 days was found to be significantly lower ($p < 0.001$) in case of LipoDox® (*i.v.*) than Dox-LCNPs (*per oral*), which could be attributed to the inherent advantages of *i.v.* administered stealth nanocarriers. Of note, the results cumulatively suggest comparable therapeutic efficacy till 20 days to that of LipoDox® (*i.v.*) followed by which the efficacy of Dox-LCNPs diminishes demanding multiple dose and/or dose adjustments.

With significant enhancement in the oral anticancer efficacy of Dox-LCNPs the obvious concern of the Dox induced cardiotoxicity was also addressed. Mechanistically, Dox is reported to intercalate with DNA strands, inhibit topoisomerase II and generate reactive oxygen species (ROS), cumulatively leading to initiation of DNA damage and inhibition macromolecules synthesis (57). However, biotransformation of Dox into free radicals and subsequent interference with mitochondrial enzymes such as CoQ10, NADH dehydrogenase results into prominent weakening of cardiac tissues which is often attributed to the Dox induced cardiotoxicity (51,58,59). The ROS induction is often associated with lipid peroxidation and reduces the levels of essential enzyme such as superoxide dismutase (SOD) and Glutathione (GSH), which activates the a vicious cycle and further contributes even higher oxidative stress (60,61). The lipid peroxidation in the cardiac tissues is also associated with myocardial ischemic injury thereby affecting Na^+/K^+-ATPase activity and mitochondrial calcium activity (62). The degree of lipid peroxidation is generally measured as a function of malondialdehyde (MDA) concentration (byproduct along with polyunsaturated fatty acids). The injury in the heart also leaches lactate dehydrogenase (LDH; an energy producing enzyme) and CK-MB in the plasma leading to increased concentrations in the plasma. Therefore, all these

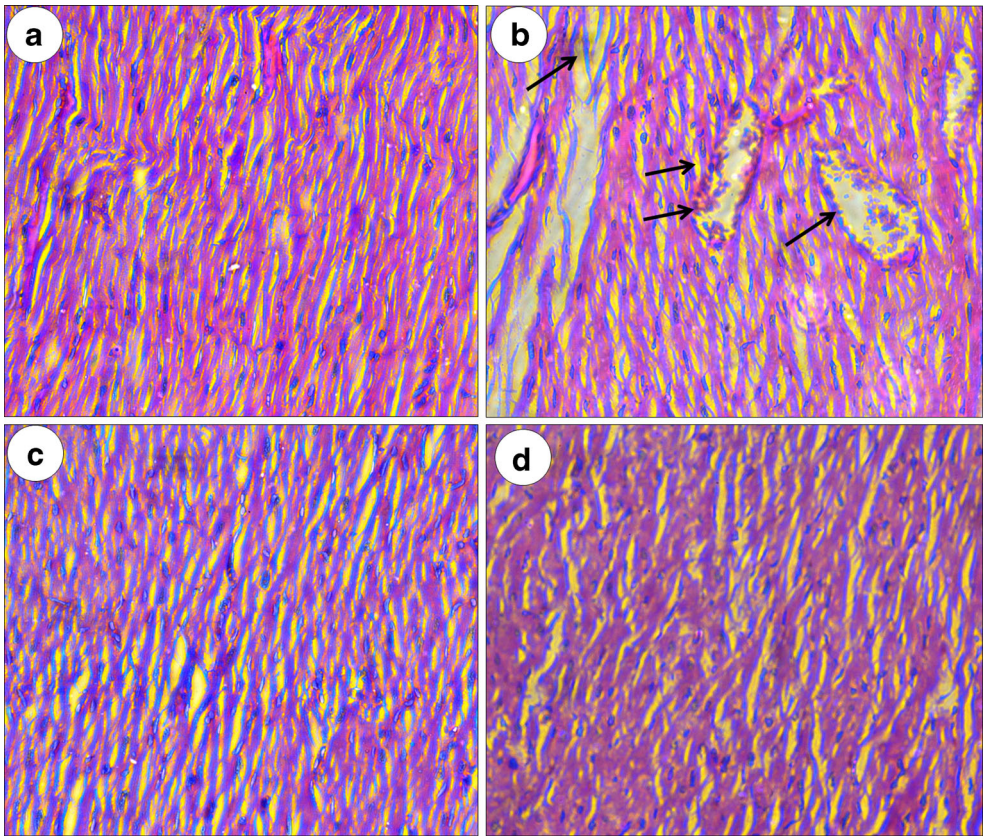

Fig. 11 Histopathology of heart tissue (**a**) control, (**b**) Adriamycin® (i.v.) the arrows depicts the vacuolization and structural changes in heart tissue (**c**) LipoDox® (i.v.), (**d**) Dox-LCNPs.

cardiotoxicity markers was utilized in the present studies (5,8,63). The levels of cardiac toxicity markers were found to be significantly ($p < 0.05$) lower in case of CK-MB, LDH and MDA and higher in case of GSH and % SOD upon administration of Dox-LCNPs (*per oral*) as compared to Adriamycin® (*i.v.*) and LipoDox (*i.v.*) (Fig. 10). Furthermore, Dox also down-regulates expression of a variety of cardiac muscle-specific proteins which are directly associated with reduced contractility of cardiomyocytes and may explain the pathologic features of myofibrillar loss in cardiac tissue (57). Therefore, histopathological examination was carried out which further revealed excessive sarcoplasmic vacuolization and severe disruption of fine structures (Fig. 11) in case of Adriamycin® (*i.v.*). In contrast, fewer myocardial morphological changes were observed in case of Dox-LCNPs which could be attributed to superior encapsulation of Dox in the LCNPs matrix. Thus, incorporation of Dox in the novel LCNPs can be a viable option for oral chemotherapy.

CONCLUSION

The employed formulation strategy has potential for improving the oral delivery of various difficult-to-deliver drugs. The principal features include simple method of preparation, sustained release profile, alternate absorption pathway, superior encapsulation of labile drugs, longer circulation half-life and preferential accumulation at target site based on enhanced permeation and retention effect. The targeting potential of the developed formulation could further be improved by implementing active targeting principles to achieve therapeutic equivalence with i.v. administered nanocarriers such as LipoDox®. In addition, multiple dose kinetics and dose adjustments can also be sought for. Successful stabilization of the prepared LCNPs by lyophilization using mannitol as cryoprotectant is also noteworthy and studies are under way for understanding the interactions at molecular level. The nuclear colocalization capabilities at intracellular level further make it potential delivery system for cancer therapeutics however mechanistic insights for same needs to be explored for better understanding. In nutshell, the said formulation strategy is promising among the field of emerging novel lipid based drug delivery system and can be explored to a greater extent for other drug delivery applications.

ACKNOWLEDGMENTS AND DISCLOSURES

Authors are thankful to Director, NIPER for providing necessary infrastructure facilities. The work was supported by Council of Scientific and Industrial Research (CSIR),

Government of India, New Delhi, India. Authors are also thankful for the technical support rendered by Mr. Rahul Mahajan.

REFERENCES

1. Rahman A, Carmichael D, Harris M, Roh JK. Comparative pharmacokinetics of free doxorubicin and doxorubicin entrapped in cardiolipin liposomes. Cancer Res. 1986;46(5):2295–9.
2. Gordon KB, Tajuddin A, Guitart J, Kuzel TM, Eramo LR, VonRoenn J. Hand-foot syndrome associated with liposome-encapsulated doxorubicin therapy. Cancer. 1995;75(8):2169–73.
3. Ryberg M, Nielsen D, Skovsgaard T, Hansen J, Jensen BV, Dombernowsky P. Epirubicin cardiotoxicity: an analysis of 469 patients with metastatic breast cancer. J Clin Oncol. 1998;16(11):3502–8.
4. Beijnen J, Van der Houwen O, Underberg W. Aspects of the degradation kinetics of doxorubicin in aqueous solution. Int J Pharm. 1986;32(2):123–31.
5. Jain AK, Swarnakar NK, Das M, Godugu C, Singh RP, Rao PR, *et al*. Augmented anticancer efficacy of doxorubicin-loaded polymeric nanoparticles after oral administration in a breast cancer induced animal model. Mol Pharm. 2011;8(4):1140–51.
6. Thanki K, Gangwal RP, Sangamwar AT, Jain S. Oral delivery of anticancer drugs: challenges and opportunities. J Control Release. 2013;170(1):15–40.
7. Kalaria DR, Sharma G, Beniwal V, Ravi Kumar MNV. Design of biodegradable nanoparticles for oral delivery of doxorubicin: in vivo pharmacokinetics and toxicity studies in rats. Pharm Res. 2009;26(3):492–501.
8. Jain S, Patil SR, Swarnakar NK, Agrawal AK. Oral delivery of doxorubicin using novel polyelectrolyte-stabilized liposomes (layersomes). Mol Pharm. 2012;9(9):2626–35.
9. Guo C, Wang J, Cao F, Lee RJ, Zhai G. Lyotropic liquid crystal systems in drug delivery. Drug Discov Today. 2010;15(23–24):1032–40.
10. Barauskas J, Johnsson M, Tiberg F. Self-assembled lipid superstructures: beyond vesicles and liposomes. Nano Lett. 2005;5(8):1615.
11. Yang D, Armitage B, Marder SR. Cubic liquid-crystalline nanoparticles. Angew Chem Int Ed Engl. 2004;43(34):4402–9.
12. Lian R, Lu Y, Qi J, Tan Y, Niu M, Guan P, *et al*. Silymarin glyceryl monooleate/poloxamer 407 liquid crystalline matrices: physical characterization and enhanced oral bioavailability. AAPS PharmSciTech. 2011;12(4):1234–40.
13. Lai J, Chen J, Lu Y, Sun J, Hu F, Yin Z, *et al*. Glyceryl monooleate/poloxamer 407 cubic nanoparticles as oral drug delivery systems: I. In vitro evaluation and enhanced oral bioavailability of the poorly water-soluble drug simvastatin. AAPS Pharm Sci Technol. 2009;10(3):960–6.
14. Tamayo-Esquivel D, Ganem-Quintanar A, Martinez AL, Navarrete-Rodriguez M, Rodriguez-Romo S, Quintanar-Guerrero D. Evaluation of the enhanced oral effect of omapatrilat-monolein nanoparticles prepared by the emulsification-diffusion method. J Nanosci Nanotechnol. 2006;6(9–10):3134–8.
15. Nguyen TH, Hanley T, Porter CJ, Larson I, Boyd BJ. Phytantriol and glyceryl monooleate cubic liquid crystalline phases as sustained-release oral drug delivery systems for poorly water-soluble drugs II. In-vivo evaluation. J Pharm Pharmacol. 2010;62(7):856–65.
16. Nguyen TH, Hanley T, Porter CJ, Larson I, Boyd BJ. Phytantriol and glyceryl monooleate cubic liquid crystalline phases as sustained-release oral drug delivery systems for poorly water soluble drugs I. Phase behaviour in physiologically-relevant media. J Pharm Pharmacol. 2010;62(7):844–55.
17. Nguyen TH, Hanley T, Porter CJ, Boyd BJ. Nanostructured liquid crystalline particles provide long duration sustained-release effect for a poorly water soluble drug after oral administration. J Control Release. 2011;153(2):180–6.
18. Final report on the safety assessment of phytantriol[1]. Int J Toxicol. 2007;26(1):107–14.
19. Lindström M, Ljusberg-Wahren H, Larsson K, Borgström B. Aqueous lipid phases of relevance to intestinal fat digestion and absorption. Lipids. 1981;16(10):749–54.
20. US Department of Agriculture. Glycerol monooleate processing. http://www.ams.usda.gov/AMSv1.0/getfile?dDocName=STELPRDC5057603 (accessed on 12 Sep, 2013).
21. Swarnakar NK, Jain V, Dubey V, Mishra D, Jain NK. Enhanced oromucosal delivery of progesterone via hexosomes. Pharm Res. 2007;24(12):2223–30.
22. Jain S, Chauhan DS, Jain AK, Swarnakar NK, Harde H, Mahajan RR, Kumar D, Valvi PK, Das M, Datir SR, et al., inventors. Stabilization of the nanodrug delivery systems by lyophilization using universal step-wise freeze drying cycle. India patent Indian Patent Application No. 2559/DEL/2011. 2011 6 September.
23. Jain S, Valvi PU, Swarnakar NK, Thanki K. Gelatin coated hybrid lipid nanoparticles for oral delivery of amphotericin B. Mol Pharm. 2012;9(9):2542–53.
24. Rosevear FB. The microscopy of the liquid crystalline neat and middle phases of soaps and detergents. J Am Oil Chem Soc. 1954;31:628–39.
25. Jain S, Kumar D, Swarnakar NK, Thanki K. Polyelectrolyte stabilized multilayered liposomes for oral delivery of paclitaxel. Biomaterials. 2012;33(28):6758–68.
26. ICH Q1A(R2): stability testing of new drug substances and products Q1A(R2), ICH harmonized tripartite guideline; Step 4 version: February 6, 2003.
27. Costa P, Sousa Lobo JM. Modeling and comparison of dissolution profiles. Eur J Pharm Sci. 2001;13(2):123–33.
28. Sharma M, Agrawal SK, Sharma PR, Chadha BS, Khosla MK, Saxena AK. Cytotoxic and apoptotic activity of essential oil from Ocimumviride towards COLO 205 cells. Food Chem Toxicol. 2010;48(1):336–44.
29. Upadhyay KK, Bhatt AN, Mishra AK, Dwarakanath BS, Jain S, Schatz C, *et al*. The intracellular drug delivery and anti tumor activity of doxorubicin loaded poly ([gamma]-benzyl l-glutamate)-b-hyaluronan polymersomes. Biomaterials. 2010;31(10):2882–92.
30. Jain V, Swarnakar NK, Mishra PR, Verma A, Kaul A, Mishra AK, *et al*. Paclitaxel loaded PEGylated gleceryl monooleate based nanoparticulate carriers in chemotherapy. Biomaterials. 2012;33(29):7206–20.
31. Putnam CD, Hammel M, Hura GL, Tainer JA. X-ray solution scattering (SAXS) combined with crystallography and computation: defining accurate macromolecular structures, conformations and assemblies in solution. Q Rev Biophys. 2007;40(3):191–285.
32. Dong YD, Larson I, Hanley T, Boyd BJ. Bulk and dispersed aqueous phase behavior of phytantriol: effect of vitamin E acetate and F127 polymer on liquid crystal nanostructure. Langmuir. 2006;22(23):9512–8.
33. Muller F, Salonen A, Glatter O. Phase behavior of Phytantriol/water bicontinuous cubic Pn3m cubosomes stabilized by Laponite disc-like particles. J Colloid Interface Sci. 2010;342(2):392–8.
34. Wubeante YA, Garkhal K, Neeraj K. Doxorubicin-loaded $(PEG)_3$-PLA nanopolymersomes: effect of solvents and process parameters on formulation development and in vitro study. Mol Pharm. 2011;8:466–78.
35. Spicer PT, Hayden KL, Lynch ML, Ofori-Boateng A, Burns JL. Novel process for producing cubic liquid crystalline nanoparticles (cubosomes). Langmuir. 2001;17(19):5748–56.

36. Friberg SE, Yang H, Fei L, Sadasivan S, Rasmussen DH, Aikens PA. Preparation of vesicles from hydrotrope solutions. J Dispers Sci Technol. 1998;19(1):19–30.
37. Johnsson M, Lam Y, Barauskas J, Tiberg F. Aqueous phase behavior and dispersed nanoparticles of diglycerol monooleate/glycerol dioleate mixtures. Langmuir. 2005;21(11):5159–65.
38. Technical Bulletin, Pluronic® block copolymer NF Grades (Poloxamer NF Grades). [26 June 2013].
39. Jain AK, Swarnakar NK, Godugu C, Singh RP, Jain S. The effect of the oral administration of polymeric nanoparticles on the efficacy and toxicity of tamoxifen. Biomaterials. 2011;32:503–15.
40. Jain S, Mistry MA, Swarnakar NK. Enhanced dermal delivery of acyclovir using solid lipid nanoparticles. Drug Deliv Transl Res. 2011;1(5):395–406.
41. Ito T, Sun L, Bevan MA, Crooks RM. Comparison of nanoparticle size and electrophoretic mobility measurements using a carbon-nanotube-based coulter counter, dynamic light scattering, transmission electron microscopy, and phase analysis light scattering. Langmuir. 2004;20(16):6940–5.
42. Hyde ST. Identification of lyotropic liquid crystalline mesophases. In: Holmberg K, editor. Handbook of applied surface and colloid chemistry. J Wiley & Sons; 2001. p. 299–332.
43. Alexandridis P, Olsson U, Lindman B. A record nine different phases (four cubic, two hexagonal, and one lamellar lyotropic liquid crystalline and two micellar solutions) in a ternary isothermal system of an amphiphilic block copolymer and selective solvents (water and oil). Langmuir. 1998;14(10):2627–38.
44. Libster D, Aserin A, Wachtel E, Shoham G, Garti N. An HII liquid crystal-based delivery system for cyclosporin A: physical characterization. J Colloid Interface Sci. 2007;308(2):514–24.
45. Amar-Yuli I, Wachtel E, Shoshan EB, Danino D, Aserin A, Garti N. Hexosome and hexagonal phases mediated by hydration and polymeric stabilizer. Langmuir. 2007;23(7):3637–45.
46. Lee KW, Nguyen TH, Hanley T, Boyd BJ. Nanostructure of liquid crystalline matrix determines in vitro sustained release and in vivo oral absorption kinetics for hydrophilic model drugs. Int J Pharm. 2009;365(1–2):190–9.
47. Rudra A, Deepa RM, Ghosh MK, Ghosh S, Mukherjee B. Doxorubicin-loaded phosphatidylethanolamine-conjugated nanoliposomes: in vitro characterization and their accumulation in liver, kidneys, and lungs in rats. Int J Nanomedicine. 2010;5:811.
48. Zeng N, Gao X, Hu Q, Song Q, Xia H, Liu Z, *et al*. Lipid-based liquid crystalline nanoparticles as oral drug delivery vehicles for poorly water-soluble drugs: cellular interaction and in vivo absorption. Int J Nanomedicine. 2012;7:3703–18.
49. Muir BW, Acharya DP, Kennedy DF, Mulet X, Evans RA, Pereira SM, *et al*. Metal-free and MRI visible theranostic lyotropic liquid crystal nitroxide-based nanoparticles. Biomaterials. 2012;33(9):2723–33.
50. Ho SY, Storch J. Common mechanisms of monoacylglycerol and fatty acid uptake by human intestinal Caco-2 cells. Am J Physiol Cell Physiol. 2001;281(4):C1106–17.
51. Swarnakar NK, Thanki K, Jain S. Effect of co-administration of CoQ10-loaded nanoparticles on the efficacy and cardiotoxicity of doxorubicin-loaded nanoparticles. RSC Adv. 2013;3:14671–85.
52. Gaymalov ZZ, Yang Z, Pisarev VM, Alakhov VY, Kabanov AV. The effect of the nonionic block copolymer pluronic P85 on gene expression in mouse muscle and antigen-presenting cells. Biomaterials. 2009;30(6):1232–45.
53. Kabanov AV, Lemieux P, Vinogradov S, Alakhov V. Pluronic block copolymers: novel functional molecules for gene therapy. Adv Drug Deliv Rev. 2002;54(2):223–33.
54. Benival DM, Devarajan PV. Lipomer of doxorubicin hydrochloride for enhanced oral bioavailability. Int J Pharm. 2012;423(2):554–61.
55. Thomson A, Schoeller C, Keelan M, Smith L, Clandinin M. Lipid absorptions passing through the unstirred layers, brush-border membrane, and beyond. Can J Physiol Pharmacol. 1993;71(8):531–55.
56. Zhang Z, Ma L, Jiang S, Liu Z, Huang J, Chen L, *et al*. A self-assembled nanocarrier loading teniposide improves the oral delivery and drug concentration in tumor. J Control Release. 2013;166(1):30–7.
57. Takemura G, Fujiwara H. Doxorubicin-induced cardiomyopathy from the cardiotoxic mechanisms to management. Prog Cardiovasc Dis. 2007;49(5):330–52.
58. Li K, Sung RY, Huang WZ, Yang M, Pong NH, Lee SM, *et al*. Thrombopoietin protects against in vitro and in vivo cardiotoxicity induced by doxorubicin. Circulation. 2006;113(18):2211–20.
59. Vasquez-Vivar J, Martasek P, Hogg N, Masters BS, Pritchard Jr KA, Kalyanaraman B. Endothelial nitric oxide synthase-dependent superoxide generation from adriamycin. Biochemistry. 1997;36(38):11293–7.
60. Singal PK, Deally CM, Weinberg LE. Subcellular effects of adriamycin in the heart: a concise review. J Mol Cell Cardiol. 1987;19(8):817–28.
61. Odom AL, Hatwig CA, Stanley JS, Benson AM. Biochemical determinants of Adriamycin toxicity in mouse liver, heart and intestine. Biochem Pharmacol. 1992;43(4):831–6.
62. Rustenbeck I, Lenzen S. Regulation of transmembrane ion transport by reaction products of phospholipase A2. II. Effects of arachidonic acid and other fatty acids on mitochondrial Ca2+ transport. Biochim Biophys Acta. 1989;982(1):147–55.
63. Si K, Liu J, He L, Li X, Gou W, Liu C. Caulophine protects cardiomyocytes from oxidative and ischemic injury. J Pharmacol Sci. 2010;113(4):368–77.